Biol. Cybern. 73, 357–366 (1995)

Biological Cybernetics

Electroencephalogram and visual evoked potential generation in a mathematical model of coupled cortical columns

Ben H. Jansen, Vincent G. Rit

Department of Electrical and Computer Engineering, and Bioengineering Research Center, University of Houston, Houston, TX 77204-4793, USA

Received: 30 August 1994/Accepted in revised form: 2 May 1995

Abstract. This study deals with neurophysiologically based models simulating electrical brain activity (i.e., the electroencephalogram or EEG, and evoked potentials or EPs). A previously developed lumped-parameter model of a single cortical column was implemented using a more accurate computational procedure. Anatomically acceptable values for the various model parameters were determined, and a multi-dimensional exploration of the model parameter-space was conducted. It was found that the model could produce a large variety of EEG-like waveforms and rhythms. Coupling two models, with delays in the interconnections to simulate the synaptic connections within and between cortical areas, made it possible to replicate the spatial distribution of alpha and beta activity. EPs were simulated by presenting pulses to the input of the coupled models. In general, the responses were more realistic than those produced using a single model. Our simulations also suggest that the scalp-recorded EP is at least partially due to a phase reordering of the ongoing activity.

1 Introduction

The electroencephalogram (EEG) is a recording of the spontaneous electrical activity of the brain recorded from surface electrodes placed on the scalp (Martin 1985). An evoked potential (EP) is a specific change in the ongoing EEG resulting from stimulation of a sensory pathway. The EEG and EP result mainly from extracellular current flow associated with summed postsynaptic potentials in synchronously activated, vertically oriented neurons.

The complexity of the EEG signal reflects the intricate cortical structures which produce it. In order to study the latter, various mathematical models have been developed to simulate electrical brain activity (see, for example, Freeman 1987; Lopes da Silva et al. 1976). The concept of a neuronal model makes it possible to reduce the complexity of cortical connections to relatively simple circuits. If the model parameters are based on anatomical data, such as the number of synapses or the excitability of neurons, then it is possible to test their respective role and influence.

The present study deals with the further development and exploration of a neurophysiologically based model of a cortical column, proposed by Jansen et al. (1993). First, a thorough evaluation of the effects brought about by variations in the parameters of the postsynaptic potential (PSP) functions and potential-to-pulse density transformation defining the model were conducted to explore the different kinds of activities a single model could produce. Next, we investigated to what degree the various components of the scalp-recorded visual evoked potential (VEP) are due to (1) the arrival of the specific afferent activity associated with the visual stimulus and/or (2) interaction between cortical areas.

Section 2 presents a brief review of the model on which the present study is based, followed by a presentation of the double-column model, and a discussion of the parameter settings. The spontaneous and evoked activities that such a model may produce are presented in Sect. 3. A discussion concludes this paper.

2 EEG and EP modeling

2.1 Single-column model

The mechanisms of oscillation generation in the brain have been proven to be nonlinear, both in cats (Kawashima et al. 1983; Shibagaki et al. 1985) and in humans (Watanabe and Shikita 1981). Hence, nonlinear models should be used to describe cortical activity. The present study deals with the further development and exploration of a nonlinear model of a cortical column described by Jansen et al. (1993). This model, in turn, is based upon Lopes da Silva's lumped parameter model (Lopes da Silva et al. 1974, 1976; Rotterdam et al. 1982). The cortical column is modeled by a population of 'feedforward' pyramidal cells, receiving inhibitory and excitatory feedback from local interneurons (i.e., other

Correspondence to: B. H. Jansen

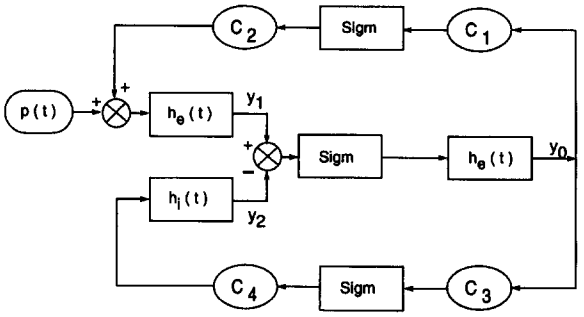

Fig. 1. Simplified model for cortical alpha generation

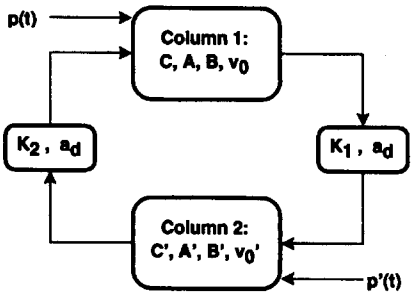

Fig. 2. Schematic diagram of the double-column model

pyramidal, stellate or basket cells residing in the same column) and excitatory input from neighboring or more distant columns (Fig. 1). The latter input is represented by a pulse density $p(t)$ which can be any arbitrary function, including white noise (see Sect. 2.2 for further details).

Each of the neuron populations is modeled by two blocks. The first block transforms the average pulse density of action potentials coming to the population of neurons into an average postsynaptic membrane potential which can either be excitatory or inhibitory. This block is referred to as the PSP block and represents a linear transformation with an impulse response given by

$$h_e(t) = \begin{cases} Aat\,e^{-at} & t \geqslant 0 \\ 0 & t < 0 \end{cases} \tag{1}$$

for the excitatory case, and

$$h_i(t) = \begin{cases} Bbt\,e^{-at} & t \geqslant 0 \\ 0 & t < 0 \end{cases} \tag{2}$$

for the inhibitory case. A and B determine the maximum amplitude of the excitatory and inhibitory PSP (EPSP and IPSP), respectively, and a and b are the lumped representation of the sum of the reciprocal of the time constant of passive membrane and all other spatially distributed delays in the dendritic network. The second block transforms the average membrane potential of a population of neurons into an average pulse density of action potentials fired by the neurons. This transformation is described by a sigmoid function of the form

$$\mathrm{Sigm}(v) = 2e_0/[1 + e^{r(v_0 - v)}] \tag{3}$$

which is a simplified, but identically behaving version of the transformation presented in Jansen et al. (1993). Here, e_0 determines the maximum firing rate of the neural population, v_0 the PSP for which a 50% firing rate is achieved, and r the steepness of the sigmoidal transformation.

The interaction between the pyramidal cells and the excitatory and inhibitory interneurons is characterized by the four connectivity constants C_1 through C_4, which account for the total number of synapses established by interneurons onto the axons and dendrites of the neurons constituting the cortical column. [In the model originally presented in Jansen et al. (1993), there was an additional branch, active only during processing of external stimuli, representing the supplementary excitation due to non-specific afferent inputs. The effect of this branch is expected to be replicated by the interaction between coupled models.]

Each PSP block introduces two differential equations of the form

$$\ddot{y}(t) = Aax(t) - 2a\dot{y}(t) - a^2 y(t) \tag{4}$$

which can be rewritten as

$$\left.\begin{aligned} \dot{y}(t) &= z(t) \\ \dot{z}(t) &= Aax(t) - 2az(t) - a^2 y(t) \end{aligned}\right\} \tag{5}$$

where $x(t)$ and $y(t)$ are the input and output signals, respectively. Using (5) we obtain the following set of six differential equations to describe the model:

$$\left.\begin{aligned} \dot{y}_0(t) &= y_3(t) \\ \dot{y}_3(t) &= Aa\ \mathrm{Sigm}[y_1(t) - y_2(t)] - 2ay_3(t) - a^2 y_0(t) \\ \dot{y}_1(t) &= y_4(t) \\ \dot{y}_4(t) &= Aa\{p(t) + C_2\,\mathrm{Sigm}[C_1 y_0(t)]\} \\ &\quad - 2ay_4(t) - a^2 y_1(t) \\ \dot{y}_2(t) &= y_5(t) \\ \dot{y}_5(t) &= Bb\{C_4\,\mathrm{Sigm}[C_3 y_0(t)]\} - 2by_5(t) - b^2 y_2(t) \end{aligned}\right\} \tag{6}$$

where y_0, y_1, and y_2 are the outputs of the three PSP blocks, respectively. These differential equations were solved using an integration method based on the Fehlberg fourth-fifth order Runge-Kutta method.

2.2 Double-column model

The hypothesis that certain VEP components are due to an interaction between two or more cortical columns was explored using two coupled model columns. Both columns are based on (6), but the system parameters (e.g., A, B and v_0) can be different for each column. Each column is fed by two inputs: an external one, which can be different for each column, and the output of the other column. Two connectivity constants, K_1 and K_2, attenuate the output of a column before it is fed to the other. In some experiments, a delay, a_d, will also be incorporated in these factors. The resulting double model is represented schematically in Fig. 2.

Typically, one of the two columns in the double-column model may represent the visual cortex, while the second one models the prefrontal cortex. We will assume that the same cortical column model can be used for the visual and prefrontal cortex. This assumption is supported by the fact that the basic neuronal architecture of the cortex is similar throughout its areas (Cynader et al. 1988; Gilbert et al. 1988). However, the proportions of cell types differ from one cortical area to the next. These differences will be represented by a different setting of the model parameter values. The prefrontal cortex typically displays beta activity (Martin 1985). The various parameters of the column will be set so that the column produces such an activity when the input is random noise. [The many projections of the thalamus to the prefrontal cortex, which have been described in recent articles by Barbas et al. (1991) and Tanibuchi (1992), substantiate the assumption of a random-noise input.] The column representing the visual cortex will be made to generate alpha activity when receiving random input. The specific parameter values will be determined on the basis of the outcome of the exploration of the single-column parameter-space.

The cortical columns located in area 17 are linked to the prefrontal cortex via two other cortical areas: the prestriate cortex (areas 18 and 19), and the inferotemporal cortex. Hence at least three neurons are necessary to account for the pathways of the processing of a visual stimulus by the prefrontal cortex and three more for the feedback to the occipital visual cortex. The delays are modeled by linear transformations similar to $h_e(t)$, defined in Eq. 1, but with a latency 3 times longer. This latency is inversely proportional to the $h_e(t)$ parameter a; hence the intercolumn delay will be modeled by

$$h_d(t) = \begin{cases} A a_d t e^{-a_d t} & t \geqslant 0 \\ 0 & t < 0 \end{cases} \tag{7}$$

where $a_d \approx a/3$.

The analytical description of such a double-column model obviously requires twice as many variables as for a single column. Three of the new variables, i.e., y_6, y_7, and y_8, are used in the second column, and are equivalent to y_0, y_1, and y_2, respectively. Four additional variables are required to represent the delay blocks in the two intercolumn branches: y_{12}, y_{13}, y_{14}, and y_{15}. The variables y_{12} and y_{13} are the outputs of the EPSP blocks added to the branches linking column 1 to column 2 and column 2 to column 1, respectively. Hence, the following set of equations defining the double-column model is obtained:

$$\left.\begin{aligned}
\dot{y}_0(t) &= y_3(t) \\
\dot{y}_3(t) &= Aa\,\mathrm{Sigm}[y_1(t) - y_2(t)] - 2a y_3(t) - a^2 y_0(t) \\
\dot{y}_1(t) &= y_4(t) \\
\dot{y}_4(t) &= Aa\{p(t) + C_2\,\mathrm{Sigm}[C_1 y_0(t)] + K_2 y_{13}\} \\
&\quad - 2a y_4(t) - a^2 y_1(t) \\
\dot{y}_2(t) &= y_5(t) \\
\dot{y}_5(t) &= Bb\{C_4\,\mathrm{Sigm}[C_3 y_0(t)]\} - 2b y_5(t) - b^2 y_2(t) \\
\dot{y}_6(t) &= y_9(t) \\
\dot{y}_9(t) &= A'a\,\mathrm{Sigm}[y_7(t) - y_8(t)] - 2a y_9(t) - a^2 y_6(t) \\
\dot{y}_7(t) &= y_{10}(t) \\
\dot{y}_{10}(t) &= A'a\{p'(t) + C_2'\,\mathrm{Sigm}[C_1' y_6(t)] + K_1 y_{12}\} \\
&\quad - 2a y_{10}(t) - a^2 y_7(t) \\
\dot{y}_8(t) &= y_{11}(t) \\
\dot{y}_{11}(t) &= B'b\{C_4'\,\mathrm{Sigm}[C_3' y_6(t)]\} - 2b y_{11}(t) - b^2 y_8(t) \\
\dot{y}_{12}(t) &= y_{14}(t) \\
\dot{y}_{14}(t) &= A'a_d\,\mathrm{Sigm}[y_1(t) - y_2(t)] \\
&\quad - 2a_d y_{14}(t) - a^2 y_{12}(t) \\
\dot{y}_{13}(t) &= y_{15}(t) \\
\dot{y}_{15}(t) &= A'a_d\,\mathrm{Sigm}[y_7(t) - y_8(t)] \\
&\quad - 2a_d y_{15}(t) - a^2 y_{13}(t)
\end{aligned}\right\} \tag{8}$$

where the parameters of the second column that are different from the corresponding parameters of the first column are indicated by a prime.

2.3 Model parameters

A literature review uncovered a number of useful relationships between the connectivity constants C_1 to C_4. These constants are proportional to the average number of synapses between the pyramidal cells and the excitatory and inhibitory feedback elements. Specifically, C_1 represents the number of synapses made by the feedforward neurons to the dendrites of the excitatory feedback loop; C_2 is proportional to the number of synapses made by the excitatory feedback loop to the dendrites of the feedforward neurons (typically, such counts include synapses of a thalamic origin, indicated here by C_2'); C_3 stands for the number of synapses made by the feedforward neurons to the dendrites of the inhibitory feedback loop; and C_4 is proportional to the number of synapses made by the inhibitory feedback loop to the dendrites of the feedforward neurons.

Studies of the visual cortex pyramidal cell of a mouse (Braitenberg and Schüz 1991) suggest that

$$C_1 + C_3 = C_2 + C_2' + C_4 \tag{9}$$

Elhanany and White (1990) found that in the mouse somato-motor cortex, a pyramidal cell axon would make 87% of its synapses on spines and 13% on shafts. It has been observed (White 1989) that a synapse made onto a spine is onto an excitatory (pyramidal) cell, but that a synapse onto a shaft is equally likely to be on an excitatory or an inhibitory cell. Hence, about 6.5% of the synapses made by a pyramidal cell are inhibitory. Therefore,

$$C_3/(C_1 + C_3) = 6.5/100 \tag{10}$$

Liu et al. (1991) established that 80% of the synapses made on a pyramidal cell dendrite in the cat motor cortex were of the excitatory type, hence

$$(C_2 + C'_2)/[(C_2 + C'_2) + C_4] = 0.8 \tag{11}$$

Most of the excitatory cells in the visual cortex are pyramidal cells (Braitenberg and Schüz 1991; Larkman 1991), hence the excitatory feedback loop is composed mainly of pyramidal cells. If the population of such cells is assumed to be homogeneous with regard to synapse patterns (i.e., all pyramidal cells establish the same number of synapses with other cells), then the number of synapses made by the feedforward neurons of a cortical column on the excitatory feedback loop should be the same as the number of synapses made by the excitatory feedback loop on the feedforward neurons. This leads to

$$C_1 = C_2 + C'_2 \tag{12}$$

According to White (1986), about 20% of the asymmetrical synapses (those assumed to be of the excitatory type) in layer IV of the cortex are formed by thalamo-cortical terminals, i.e.,

$$C'_2/(C_2 + C'_2) = 0.2 \Rightarrow C'_2 = C_2/4 \tag{13}$$

Substituting (13) in (12), one obtains

$$C_2/C_1 = 0.8 \tag{14}$$

From (9) and (12) we get

$$C_3 = C_4 \tag{15}$$

The relationship between the number of synapses on the excitatory and inhibitory feedback loops is more ambiguous. For example, (10) yields $C_1 = 14.4C_3$, while substituting (12) and (15) in (11) yields $C_1 = 4C_3$. These discrepancies may be due to the different biological materials used in the synapse counts, the variability associated with such studies, and the actual differences between pyramidal cells throughout the visual cortex. We will assume that $C_1 = 4C_3$, resulting in

$$C_1 = C_2/0.8 = 4C_3 = 4C_4 \tag{16}$$

These relationships allow us to represent each of the four connectivity constants as a fraction of one constant, C. Specifically, by selecting $C = C_1$, we obtain $C_2 = 0.8C$; $C_3 = 0.25C$; and $C_4 = 0.25C$. The variable C is one of the parameters most likely to vary under different physiological constraints, because it accounts for synaptic phenomena such as neurotransmitter depletion, which are common and can have drastic consequences.

The A and B parameters of the PSP functions are proportional to the amplitude of the PSP. It is suggested that $A = 3.25$ mV and $B = 22$ mV (van Rotterdam et al. 1982). Certain neuropeptides modify the amplitude of the PSPs (Dodt et al. 1991), hence A and B have to be granted a degree of freedom. The a and b parameters of the PSP blocks are inversely proportional to the duration of the PSP. These are less likely to vary over relatively short periods, and therefore will be set to the same fixed values as used before (Jansen et al. 1993), namely, $a = 100\ s^{-1}$ and $b = 50\ s^{-1}$. The PSP blocks accounting for the delays in the intercolumn branches in the double-column model will use the same A as the other PSP blocks, but $a_d = 30\ s^{-1}$.

The excitability of cortical neurons is also very sensitive to a variety of substances (McCormick et al. 1991; Albus et al. 1992; Nowicky et al. 1992). Hence the effect of varying v_0, which accounts for the firing threshold in (3), will be studied, but in most cases we will use $v_0 = 6$ mV, as suggested by Freeman (1987). The remaining parameters in (3) will remain fixed, with $e_0 = 2.5\ s^{-1}$ and $r = 0.56\ mV^{-1}$.

Following our previous study (Jansen et al. 1993), the random white noise input $p(t)$ will have an amplitude varying between 120 and 320 pulses per second.

3 Results

The first two parts of this section present the types of spontaneous activity produced by a single cortical column, and by two mutually coupled models, respectively. The third part presents the evoked activity generated using the double-column model.

3.1 Spontaneous activity in a single-column model

The literature suggests that the model produces oscillating output if $A = 3.25$ mV (van Rotterdam et al. 1982), $B = 22$ mV (van Rotterdam et al. 1982), and $v_0 = 6$ mV (Freeman 1987). No such information can be found for the lumped connectivity constant parameter C. The effect of this parameter was explored experimentally, using the other parameters set to the aforementioned values and a random input uniformly distributed between 120 and 320 pulses per second. Varying C led to the different kinds of output presented in Fig. 3. As can be seen, increasing C results in an output evolving from noise to noisy alpha-like activity, to well-defined alpha-like activity (at $C = 135$), and a quasi-periodic signal resembling spike-wave complexes with a frequency getting lower until it reaches zero and finally becomes noise-like.

The fact that alpha-like activity was seen for $C = 135$ led us to define the following set of *standard values* for the model parameters of the visual cortical column:

$$\left.\begin{aligned} A &= 3.25 \\ B &= 22 \\ C &= 135 \\ v_0 &= 6 \end{aligned}\right\} \tag{17}$$

Similar activity as presented in Fig. 3 was found when either A, B or v_0 was independently increased from a low value to a high one. This can be explained as follows. The third panel from the top in Fig. 3 demonstrates that the output level is between 5 and 10 when the standard values are used, i.e., in the linear range of the sigmoid defining the potential-to-density transformation. If the feedback is increased (by increasing A or decreasing B),

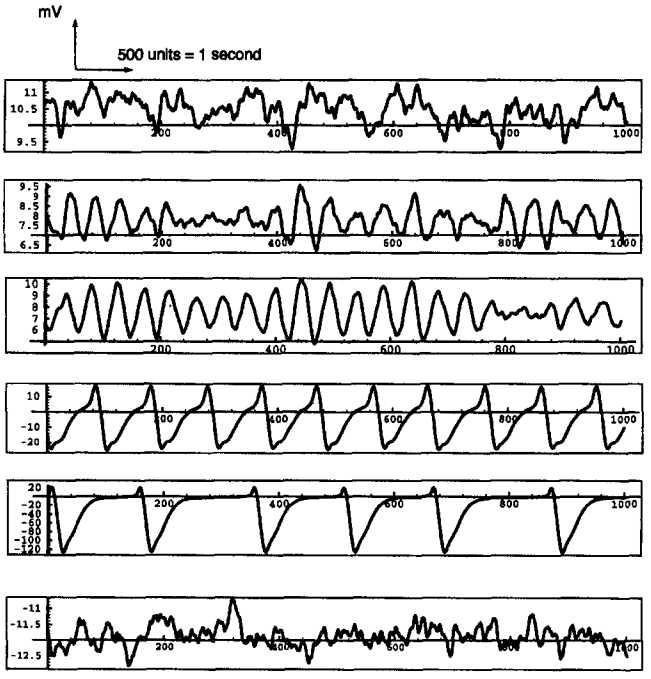

Fig. 3. Two seconds of the model's output when the lumped connectivity constant C equals (from top to bottom) 68, 128, 135, 270, 675, and 1350, respectively. The input is uniformly distributed random noise

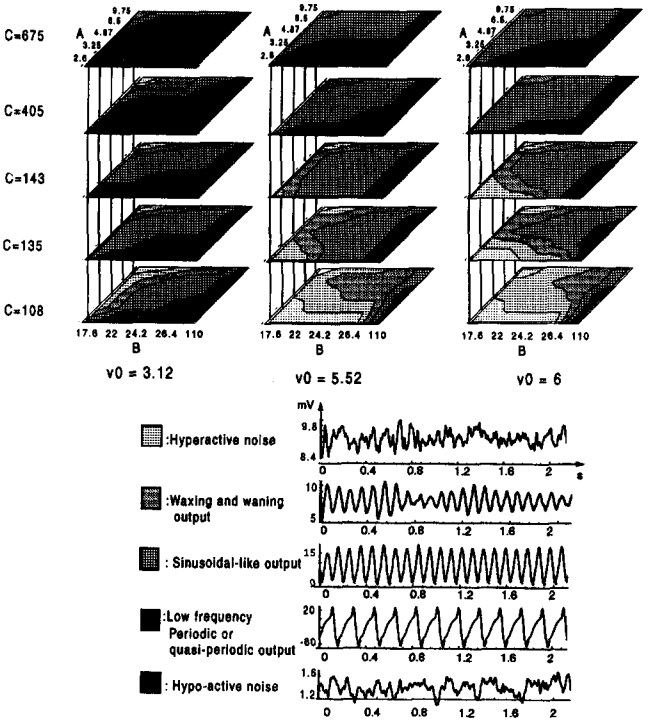

Fig. 4. Exploration of the four-dimensional parameter-space for one column. The input is random noise

then the global level of the input (i.e., the random input added to the feedback level) will be in the upper saturating region of the sigmoid, bringing about a constant output of the sigmoid transformation, hence a constant feedback, hence no oscillations. If, on the other hand, the feedback is decreased (by decreasing A or increasing B), then the global level of the input will be in the lower saturating region of the sigmoid, bringing about a null output of the sigmoid transformation, hence a null feedback, hence a global input reduced to the random input leading to nonoscillatory behavior as presented in Fig. 3 for a low value of C. Changing the value of v_0 corresponds to shifting the range of the linear part of the sigmoid, eventually leading to one of the two aforementioned nonoscillatory cases.

A more detailed exploration of the four-dimensional parameter-space (A, B, C and v_0) was done around values for which alpha and other periodic activity was generated. Specifically, A was varied between 2.6 and 9.75 mV, B ranged from 17.6 to 110 mV, C from 108 to 675, and v_0 was either 3.12, 5.52, or 6.0 mV. The results are presented in Fig. 4, which shows that the region of the parameter-space where the system oscillates is bounded by two regions of noise. An increase or decrease in any parameter from a point of oscillation will eventually lead to a nonoscillatory mode. The two aforementioned regions of noise never touch one another. One is characteristic of a relatively high B parameter compared with A, i.e., a low excitatory feedback, and will be referred to as hypoactive noise. The other noise region will be denoted as hyperactive noise, and resembles the fast, low-amplitude EEG seen during mental activity ('beta activity'). Going from the hypoactive noise region to the hyperactive one, a path in the parameter-space would cross the regions always in the same order: starting at a low-frequency quasi-periodic signal (2–3 Hz), via a higher-frequency quasi-periodic signal (8–9 Hz), and alpha activity, to a noisy alpha, and, finally, to the hyperactive noise. It is interesting to note, however, that for $C = 135$ and $v_0 = 6$, the region for which the system oscillates forms a valley; for a B value of less than 22, an increase or a decrease in A will lead to hyperactive noise, the hypoactive region being reachable for high B values only.

3.2 Spontaneous activity in a double-column model

Simulation of the interactions of two columns located in the visual cortex. A double-column model was built with the parameters of both columns set to identical values. The values were chosen such that a single column produced alpha activity when receiving random input. A zero-delay was used in the intercolumn branches to mimic the short neural pathways linking columns located in the same cortical area. Both columns received uncorrelated, random, uniformly distributed inputs (between 120 and 320 pulses per second) while K_1 and K_2 were varied simultaneously between 0 and 120 in steps of 10.

As shown in Fig. 5, the model behaves symmetrically for variations in K_1 and K_2, which is predictable given the symmetry of the system, i.e., two identical columns fed with similar inputs. The results also demonstrate that, if one of the intercolumn connectivity coefficients is small ($K_i < 12$), then both columns generate a waxing and waning output. This is understandable, because the

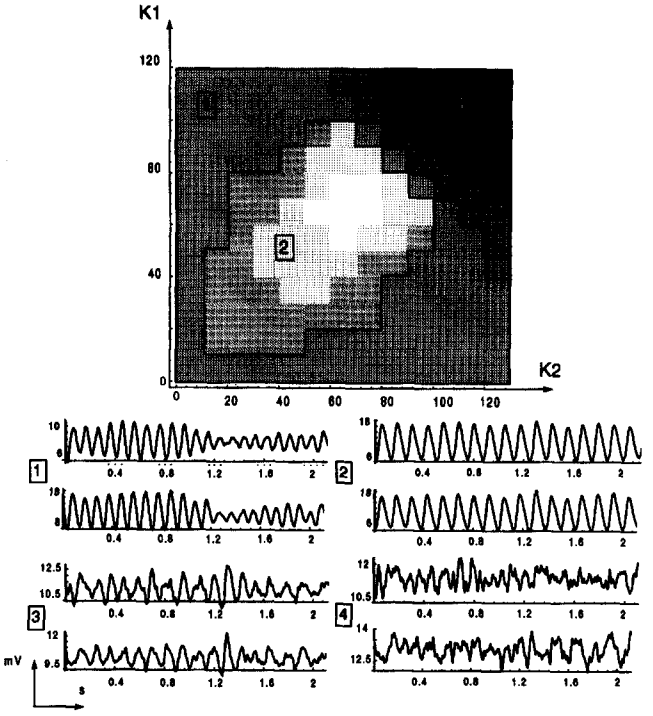

Fig. 5. Four different classes of oscillatory behavior were observed for a double-column model (no delay) composed of identical columns with parameters at their standard values, and fed with uncorrelated random inputs. The parameters K_1 and K_2 are the intercolumn connectivity constants

parameters of each column have purposely been set to obtain that kind of behavior if the columns are not coupled. Synchronized activity was obtained when both K values where as small as 1.4, which demonstrates that a weak coupling between the two columns is enough to reach synchronization.

If K_1 and K_2 are jointly increased, then the symmetrical coupling between the two columns first induces a decrease in the waxing and waning of the output, which becomes almost sinusoidal. It is worthy of note that increasing the coupling up to 80 tends to shift the frequency of the synchronized outputs downwards, from 10.5 Hz to 8 Hz, whereas a further increase in the coupling from 80 to 90 brings about an increase in the output frequency. An even larger increase in K_1 and K_2 provokes a saturation of the columns. Accordingly, their outputs look more and more noisy, until desynchronization is reached and the columns produce a noise-like signal. This global behavior corroborates the single-column study: a zero-coupling case corresponds to a single column with the (A, B, C, v_0) parameters set to their standard values, hence a 10 Hz waxing and waning activity. Increasing the coupling between the two columns roughly corresponds to an increase in the excitatory feedback. As shown in Fig. 4, starting from the standard values, an increase in A, while keeping the other parameters fixed, leads to outputs that are first waxing and waning, proceed to become sinusoidal-like, once more exhibit waxing and waning, and eventually become noise-like.

Simulation of the interactions of two columns located in different cortical areas. In the following experiments the parameter values for column 1 have been set to the standard set, so that it represents a column in the visual cortex. Model column 2 is supposed to represent a prefrontal column, and its parameters have been selected such that it produces beta-like activity. As can be seen from Fig. 4, beta-like activity is produced for a range of values for A, B, and C when $v_0 = 6.0$ (the standard value), and we selected arbitrarily $A' = 3.25$, $B' = 17.6$, and $C' = 108$. Both columns received uncorrelated random inputs uniformly distributed between 120 and 320 pulses per second. K_1 was varied between 0 and 8000 in steps increasing from 50 to 4000 units, while K_2 was varied from 0 to 1500 in steps of 100 to 500 units. Anatomically, the feedforward connections to the prefrontal cortex are stronger than the feedback connections to the visual cortex (Pandya and Yeterian 1990), justifying a setting of K_1 roughly one order of magnitude larger than K_2. A delay, corresponding to three synapses, was incorporated in the connections between the model columns, as discussed Sect. 2.2.

The results of the simulations are presented in Fig. 6. For small values of K_2 (< 200), the output of column 1 was of the waxing and waning type, irrespective of the value of K_1. This is consistent with the fact that the model was designed so that column 1 would produce alpha activity when it is independent. As K_2 was increased, the additional feedback progressively saturated column 1, causing the output to wax and wane more sharply, displaying more high-frequency components until it eventually resembled beta activity. The output of column 2 resembled beta activity when the column operated independently, i.e., for small K_1 and K_2. For $K_2 < 500$, increasing K_1 causes column 2 gradually to change its output from beta-like to alpha-like activity. However, for $K_2 > 700$, column 2 produced beta-like activity exclusively.

3.3 *Evoked potentials*

Simulations of evoked potentials were done on the two types of double-column model explored in the previous two subsections, namely the model with two identical columns and no delay in the intercolumn connections, and the model with the two different columns and delays in the interconnections. The double-column models received two types of input, namely random and transient activity. The random input was provided to *both* columns, and was uniformly distributed between 120 and 320 pulses per second. This input represents the 'spontaneous background' activity. A transient component, representing the impulse density attributable to a brief visual input (a flash), was added only to the input of column 1 (set to produce alpha activity when stimulated by random input). This transient is similar to the one used in Jansen et al. (1992), and is given by

$$P(t) = q(t/w)^n \, \mathrm{e}^{-t/w} \tag{18}$$

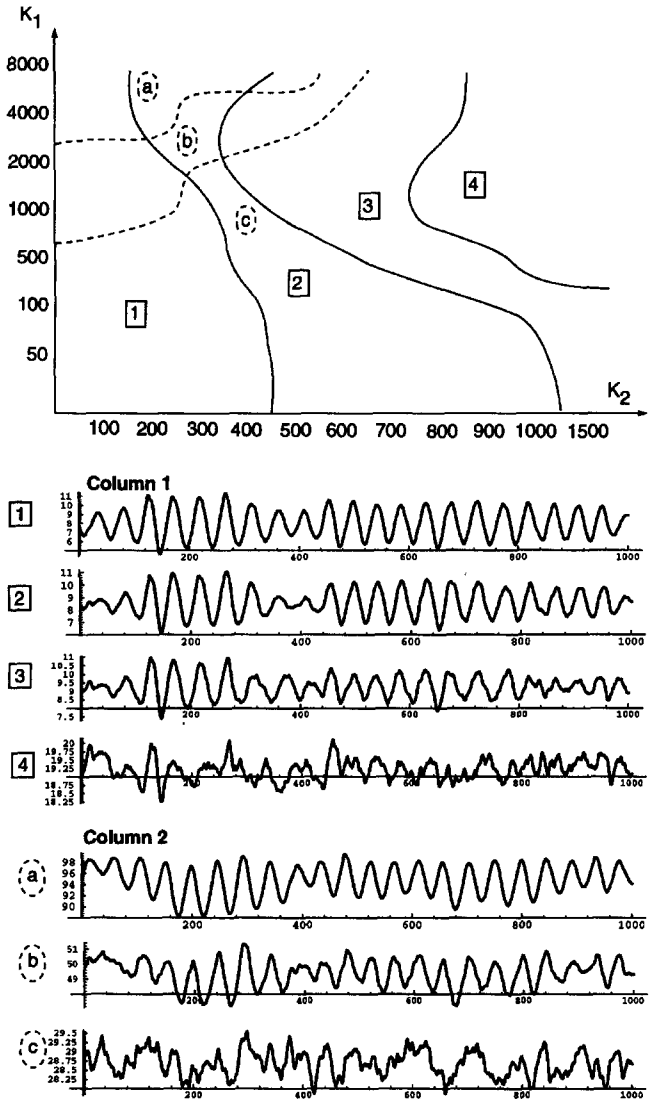

Fig. 6. Exploration of the K_1/K_2 plane for a double-column model with one column located in the visual cortex and one in the prefrontal area (delay equivalent to three synapses)

with $n = 7$, $w = 0.005$ (if t is in seconds), and $q = 0.5$. The models were run for 6 s before the stimulus was applied to avoid transient behavior, and ensemble averages of 20 or 40 single trials each were computed for each model, using a different random input for each trial. An actual scalp-recorded flash VEP is presented in Fig. 7 for comparison.

Identical columns. Experiments with two interconnected, identical models (no delays in the interconnections, and $K = K_1 = K_2$) revealed that a multicomponent response was produced for low K values (< 10) by column 1. A W shape around 100 ms after the stimulus can be observed (Fig. 8). Although it appears in certain real VEPs (Fig. 7), this feature is not the norm. Increasing K makes the response less complicated in form, until it resembles the shape of the applied input stimulus as K exceeds 100 (Fig. 8). Virtually no stimulus-related effect is seen in column 2 for any K value, although some

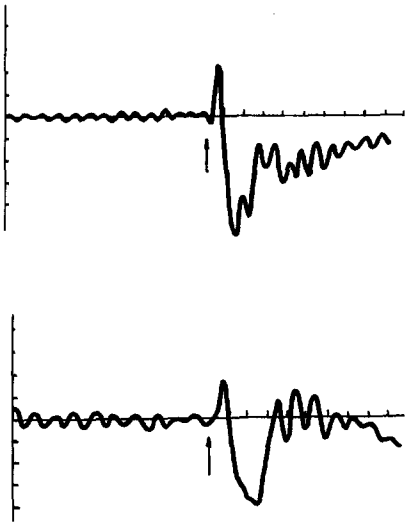

Fig. 7. Average VEPs recorded from normal volunteers. The *arrow* indicates the time of stimulation (negative up)

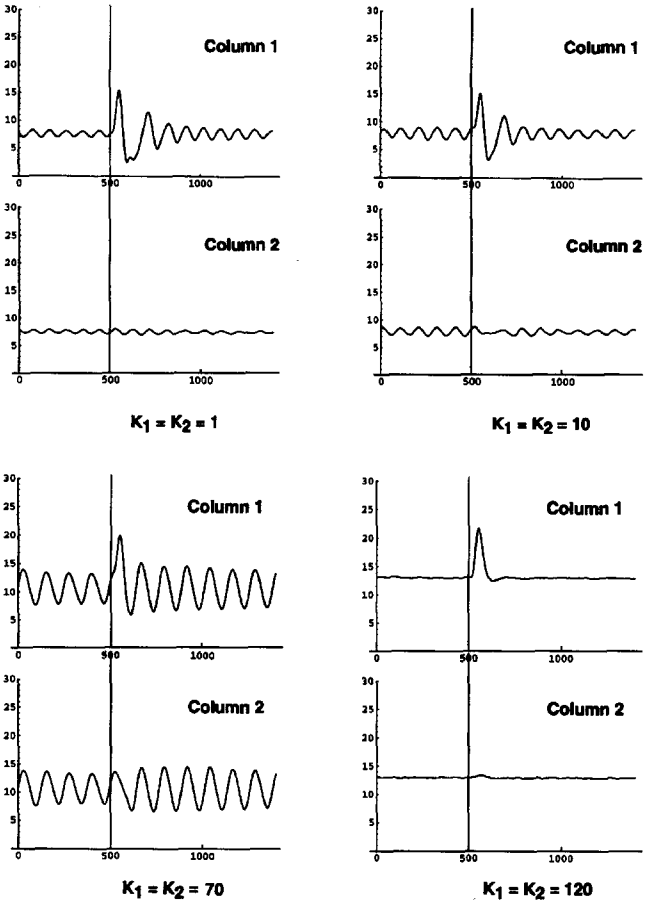

Fig. 8. Average response to a pulse, over 20 trials, of the double-column model (no delay, identical columns) to a pulse. The *vertical line* indicates the time of stimulation (negative up)

alpha attenuation appears to occur in the interval 100–200 ms after stimulation for $K = 10$, and for $K = 70$ some distortion in the poststimulus alpha activity is seen during that same period.

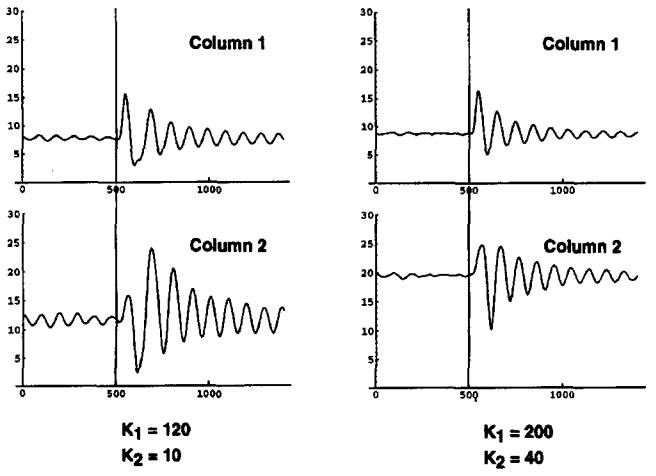

Fig. 9. Average response to a pulse, over 20 trials, of the no-delay, identical-columns model to a pulse when $K_1 \neq K_2$. The vertical line indicates the time of stimulation (negative up)

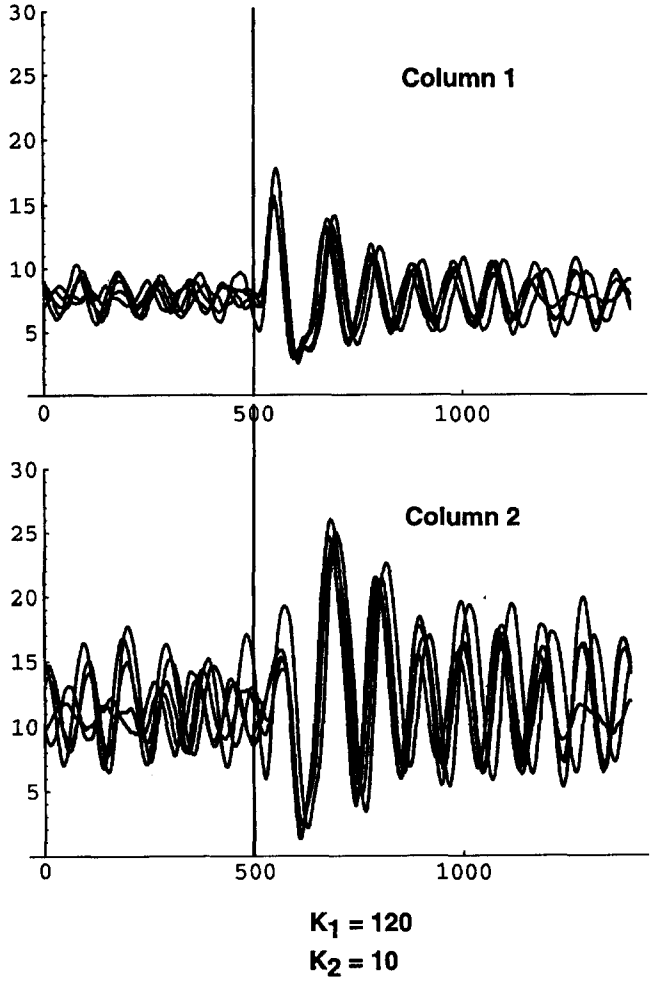

Fig. 10. Five single responses to a pulse, produced by the no-delay, identical-columns model for $K_1 = 120$ and $K_2 = 10$

A stimulus-related effect can be observed in column 2 if K_1 is made about an order of magnitude larger than K_2, as shown in Fig. 9. Under those circumstances, the averaged response resembles a damped sinusoid,

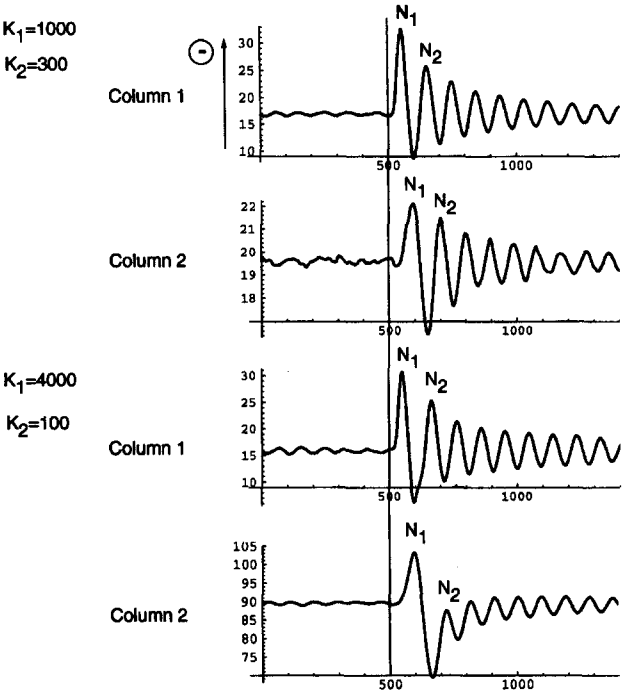

Fig. 11. Average response to a pulse, over 40 trials, of the double-column model (delay, different columns). The vertical line indicates the time of stimulation (negative up)

especially for larger values of K_1. Also, the peak-to-peak amplitude during the first 500 ms poststimulus is much larger than prestimulus. This suggests that the presentation of a single stimulus causes a phase reorganization (synchronization) of the ongoing activity, and/or a damped sinusoidal response (ringing). This issue was explored by investigating single trials. In Fig. 10 we present the first five trials used to compute the averaged response for $K_1 = 120$ and $K_2 = 10$ as shown in Fig. 9. A ringing effect is immediately apparent, but a synchronization effect can be observed as well. Specifically, the trials appear to synchronize within 50 ms of the stimulus, and start to desynchronize about 50 ms later.

Different columns. The results obtained with the double-column model, using different model parameters for each column and delays in the intercolumn branches, are presented in Fig. 11. The two examples presented are typical of the two kinds of VEPs produced by the model when K_1 is roughly one order of magnitude larger than K_2. The increased latencies of N_1 in the prefrontal columns (columns 2), as compared with the column 1 latency, are clearly visible. It should be observed that the amplitude of N_2 in the prefrontal column depends heavily on the values of the constants K_1 and K_2. For relatively low values of K_1 and K_2 (1000 and 300, respectively), the VEP produced by the system is similar to the damped sinusoidal wave already mentioned in the case of a double-column model with no delay. For different values of K_1 and K_2 (such as 4000 and 100, respectively), the system yields a new kind of VEP with a high-amplitude N_1, a very low-amplitude N_2 peak, and the

suggestion of a slow wave component typical of certain real flash VEPs (upper panel of Fig. 7). Interestingly, this slow wave component occurs in the column that does not receive the primary visual stimulus.

Removing the delay produced results that were very similar to those obtained for the model with two identical columns (presented in Fig. 9).

4 Conclusions and discussion

The model for EP generation introduced in Jansen et al. (1993) was explored in more detail and extended. A study of the four-dimensional system parameter-space demonstrated that, when fed with random noise, five typical outputs could be observed depending on the setting of the parameter values: hypoactive noise for high values of the inhibitory feedback, slow periodic activity similar to that obtained in comatose patients (Chatrian 1990), alpha activity, noisy alpha activity, and low-amplitude high-frequency activity similar to beta activity for high values of the excitatory feedback.

Coupling two identical single-column models, so as to simulate the interactions between two columns located in the visual cortex, produced in-phase oscillations. The phase locking remained, even for low values of the intercolumn connectivity constants. Persistent synchronization of neocortical activity may also be observed in patients with bilateral pontine infarcts involving the tegmentum, for instance (Daly and Markand 1990).

A second simulation involving two different columns, one representative of the visual and the other of the prefrontal cortical areas, reproduced the alpha and beta activities typically found over the visual and the prefrontal regions of the scalp.

The EP simulations suggest that the *averaged* VEP components typically seen during the first 100–200 ms are primarily due to a combination of phase reorganization and the processing of the primary afferent activity. In general, the results obtained with a double-column model were not dramatically different from those produced by a single-column model (as presented in Jansen et al. 1993). However, the addition of delays within the intercolumn branches brought about a slow wave component following P1, not seen in single-column simulations, provided that K_1 and K_2 (i.e., the intercolumn connectivity coefficients) were fairly large. Hence, cortical interaction appears to be important in the generation of later components.

It should be stressed that we do not *imply* that only two cortical columns are involved in EP production. We used a lumped parameter model of a cortical column and, therefore, one model column could be taken to represent the action of numerous actual cortical columns or even a section of the cortex.

The model presented here suffers from a problem common to all mathematical models, namely that a number of assumptions have been made in its derivation. Consequently, our model should be viewed as just one of the many possibilities as to how neuronal interactions may give rise to EEG and EP. However, most of our model parameters are related to architectural, neurochemical, and behavioral characteristics of cortical networks. Therefore, experimental verification of the model might be possible, by comparing model output with the actual EEG recorded under conditions where neuronal behavior has been selectively altered through, for example, administration of drugs.

The various counts of synapses we reviewed led to different equations between the connectivity constants. The most contentious of the ratios used to determine C is C_2/C_4 (equal to C_1/C_3). A qualitatively different outcome of our simulation experiments could have been obtained if a more accurate value of C_2/C_4 had been available. However, an accurate synaptic count might be of little value: the location and efficiency of the synapses can have an influence on the global connectivity constants at least as important as their actual number. Inhibitory neurons, for instance, are much more likely to synapse near the cell body of a pyramidal cell than are excitatory neurons (Martin 1985), producing larger PSPs. This was accounted for in our model by selecting $B > A$ (Eqs. 1 and 2). Also, it should be noted that the PSP constants A and B can compensate for any bias in the values of C_2 and C_4. Since the effect of varying A and B was studied in the four-dimensional space exploration, we can assume that a wide range of values of the ratio C_2/C_4 was explored.

In our experiments, the nonlinear potential-to-pulse density functions of the three neurons included in the pathways between visual and prefrontal areas were not implemented. Also, the two single-column models were coupled by adding the output of one column to the excitatory feedback of the other. Although intercolumn neurons are generally excitatory (Martin 1985), they can synapse on inhibitory cells as well as excitatory ones. Thus, an intercolumn reinforcement of the *inhibitory* feedback loop is possible; this case was not dealt with in our study.

We intend to improve our model along aforementioned lines. Also, we will increase the number of model columns to replicate better the complex interactions between various brain regions when processing sensory stimuli. We hope that such an expanded model will shed light on the mechanism underlying the generation of very late components, such as P300, which are often associated with cognition.

References

Albus K, Chao HH-A, Hicks TP (1992) Tachykinins preferentially excite certain complex cells in the infragranular layers of feline striate cortex. Brain Res 587:353–357

Barbas H, Henion TH, Dermon CR (1991) Diverse thalamic projections to the prefrontal cortex in the rhesus monkey. J Comp Neurol 313:65–94

Braitenberg V, Schüz A (1991) Anatomy of the cortex: statistics and geometry. Springer, Berlin Heidelberg New York

Chatrian GE (1990) Coma, other states of altered responsiveness, and brain death. In: Daly DD, Pedley TA (eds) Current practice of clinical electroencephalography, 2nd edn. Raven Press, New York, pp 425–487

Cynader MS, Andersen RA, Bruce CJ, Humphrey DR, Mountcastle VB, Niki H, Palm G, Rizzolatti G, Strick P, Suga N, Seelen W von, Zeki S (1988) Group report: general principles of cortical operation. In: Rakic P, Singer W (eds) Neurobiology of neocortex. Wiley, Chichester, pp 353–371

Daly DD, Markand OM (1990) Focal brain lesions. In: Daly DD, Pedley TA (eds) Current practice of clinical electroencephalography, 2nd edn. Raven Press, New York, pp 335–370

Dodt HU, Pawelzik H, Zieglgansberger W (1991) Actions of noradrenaline on neocortical neurons in vitro. Brain Res 545:307–311

Elhanany E, White EL (1990) Corticocortical axon collaterals. J Comp Neurol 291:43–54

Freeman WJ (1987) Simulation of chaotic EEG patterns with a dynamic model of the olfactory system. Biol Cybern 56:139–150

Gilbert CD, Bourgeois J-P, Eckhorn R, Goldman-Rakic PS, Jones EG, Krüger J, Luhmann HJ, Lund JS, Orban GA, Prince DA, Sillito AM, Somogyi P, Toyoma K, Essem DC van (1988) Group report: neuronal and synaptic organization in the cortex. In: Rakic P, Singer W (eds) Neurobiology of neocortex. Wiley, Chichester, pp 219–240

Jansen BH, Zouridakis G, Brandt ME (1993) A neurophysiologically based mathematical model of flash visual evoked potentials. Biol Cybern 68:275–283

Kawashima T, Miyake A, Yamazaki T, Watanobe S, Shikita Y (1983) An analysis of the non-linearity of the visual evoked responses of the cats. J Physiol Soc Jpn 45:453

Larkman AU (1991) Dendritic morphology of pyramidal neurones of the visual cortex of the rat. III. Spine distributions. J Comp Neurol 306:332–343

Liu XB, Zheng ZH, Xi MC, Wu CP (1991) Distribution of synapses on an intracellularly labeled small pyramidal neuron in the cat motor cortex. Anat Embryol 184:313–318

Lopes da Silva FH, Hoek A, Smits H, Zetterberg LH (1974) Model of brain rhythmic activity: the alpha rhythm of the thalamus. Kybernetik 15:27–37

Lopes da Silva FH, Rotterdam A van, Barts P, Heusden E van, Burr W (1976) Model of neuronal populations: the basic mechanism of rhythmicity. Prog Brain Res 45:281–308

Martin JH (1985) Cortical neurons, the EEG, and the mechanisms of epilepsy. In: Kandel ER, Schwartz JH (eds) Principles of neural science, 2nd edn. Elsevier, Amsterdam, pp 636–647

McCormick AD, Pape HC, Williamson A (1991) Actions of norepinephrine in the cerebral cortex and thalamus: implications for function of the central noradrenergic system. Prog Brain Res 88:293–305

Nowicky AV, Christofi G, Bindman LJ (1992) Investigation of beta-adrenergic modulation of synaptic transmission and postsynaptic induction of associative LTP in layer V neurones in slices of rat sensorimotor cortex. Neurosci Lett 137:270–273

Pandya DN, Yeterian EH (1990) Prefrontal cortex in relation to other cortical areas in rhesus monkey: architecture and connections. Prog Brain Res 85:63–94

Rotterdam A van, Lopes da Silva FH, Ende J van der, Viergever MA, Hermans AJ (1982) A model of the spatial-temporal characteristics of the alpha rhythm. Bull Math Biol 44:283–305

Shibagaki M, Kiyono S, Kawashima T, Watanabe S (1985) Non-linearity of VEPs in cerveau isolé and midpontine pretrigeminal cats. Electroencephalogr clin Neurophysiol 62:65–73

Tanibuchi I (1992) Electrophysiological and anatomical studies on thalamic medio-dorsal nucleus projections onto the prefrontal cortex in the cat. Brain Res 580:137–149

Watanabe S, Shikita S (1981) Stability of alpha rhythm. In: Yamaguchi N, Fujisawa K (eds) Recent advances in EEG and EMG data processing. Elsevier/North-Holland, Amsterdam, pp 87–94

White EL (1986) Terminations of thalamic afferents. In: Peters A, Jones EG (eds) The cerebral cortex vol 5, Sensory-motor areas and aspects of cortical connectivity. Plenum Press, New York, pp 271–289

White EL (1989) Cortical circuits. Birkhäuser, Boston